

# Fractional Order PD <sup>$\alpha$</sup> Joint Control of Legged Robots

MANUEL F. SILVA

J. A. TENREIRO MACHADO

*Department of Electrical Engineering, Institute of Engineering of Porto, Rua Dr. António Bernardino de Almeida, 4200-072 Porto, Portugal (mss@isep.ipp.pt)*

(Received 26 January 2006; accepted 15 May 2006)

*Abstract:* This paper studies a fractional order proportional and derivative controller for a hexapod robot, having legs with three DoF and joint actuators with saturation, when walking over ground with varying properties. A simulation model is developed and the robot motion is characterized in terms of several locomotion variables. Two indices measure the walking performance based on the mean absolute density of energy per unit distance travelled and on the hip trajectory errors. A set of experiments reveal the influence of different controller tunings on the proposed indices, for different locomotion conditions.

*Keywords:* Robotics, walking, control algorithms, fractional calculus, performance analysis

## 1. INTRODUCTION

Legged robots allow locomotion in terrain inaccessible to other type of vehicles, since they do not need a continuous support surface. However, the implementation of leg coordination and control schemes is more challenging than the control of wheeled or tracked robots. There is a class of walking machines for which locomotion is a natural dynamic mode. Once started on a slope, a machine of this class will settle into a steady gait, without active control or energy input (McGeer, 1990; Smith and Berkemeier, 1997), but their capabilities are quite limited. Previous studies have mainly focused on control at the leg level and leg coordination using neural networks (Tsai and Lee, 1998), fuzzy logic (Tsai et al., 1997), central pattern generators (Collins and Richmond, 1994) and subsumption architecture (Celaya and Porta, 1995). There is also a growing interest in using insect locomotion schemes to control walking robots (Ferrell, 1995).

In spite of these distinct approaches, control at the leg joint level in multi-legged robots is usually implemented through a simple proportional, integral and derivative (PID) like algorithm with position/velocity feedback. Other approaches include sliding mode control (Martins-Filho et al., 2003), computed torque control (Lee et al., 1998) and hybrid force/position control (Song et al., 1999).

The application of the theory of fractional calculus to robotics is still at the research stage, but recent progress in this area reveals promising aspects for future developments (Silva et al., 2003a). Bearing these ideas in mind, a simulation model for multi-leg loco-

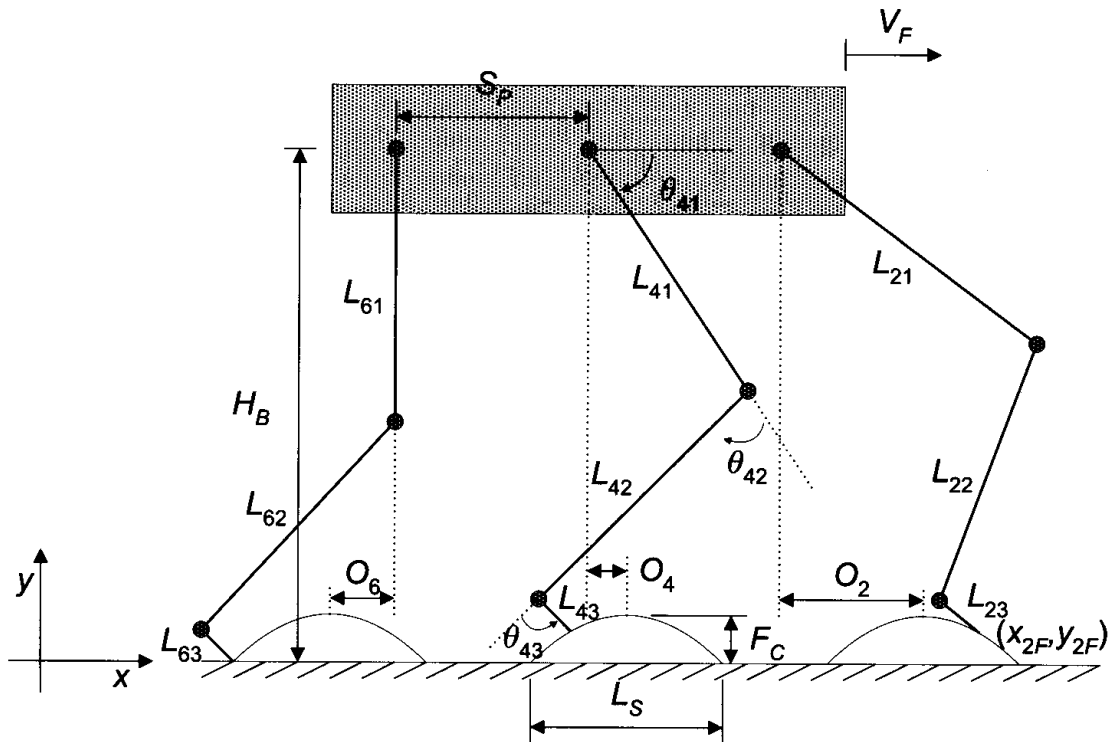


Figure 1. Coordinate system and variables that characterize the motion trajectories of the multi-legged robot.

motion systems was developed, for several periodic gaits. Based on this tool, the present study compares different fractional order proportional and derivative (FO PD $^\alpha$ ) robot controller tunings. The analysis is based on two indices, measuring the mean absolute density of energy per unit distance travelled and the hip trajectory errors during walking. The system performance is analysed for two cases: With two leg joints motor actuated while the third (ankle) joint is mechanically (passively) actuated, and with all three leg joints motor actuated. The simulations reveal the superior performance of the FO PD $^\alpha$  controller for the fractional order  $\alpha_j = 0.5$ , and the case when all leg joints are motor actuated.

The paper is organized as follows: Section two introduces the robot kinematic model and the motion planning scheme; sections three and four present the robot dynamic model and control architecture, respectively; section five formulates the optimization indices used to measure the robot's locomotion performance; section six develops a set of experiments that compare the performances of different controller tunings; and section seven outlines the main conclusions and directions for future developments.

## 2. ROBOT KINEMATICS AND TRAJECTORY PLANNING

We consider a walking system (Figure 1) with  $n = 6$  legs, equally distributed along both sides of the robot body, each having three degrees of freedom (DoF) corresponding to three rotational joints (i.e.,  $j = \{1, 2, 3\} = \{\text{hip, knee, ankle}\}$ ) (Silva et al., 2006c).

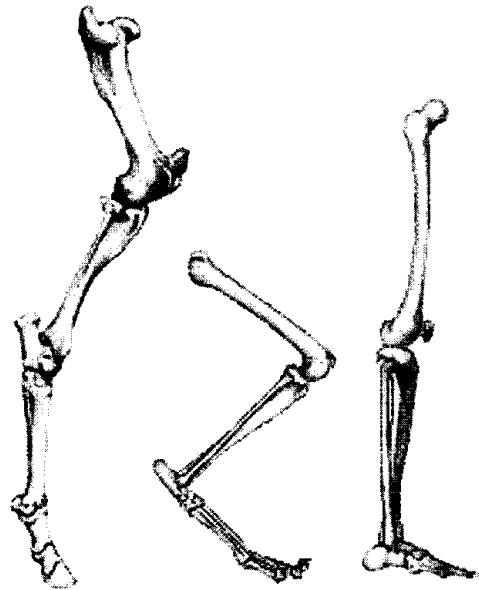


Figure 2. Different ways to place the foot on the ground (from left to right): Skeleton of the rear leg of the horse (unguligrade), cat (digitigrade) and human (plantigrade) (Alexander, 1995).

The adoption of legs with this mechanical structure stems from the fact that, irrespective of how they place the foot on the ground during locomotion (Figure 2), mammals have legs with three DoF (three segments) (Witte et al., 2001). In addition, feet play an important role in human and animal locomotion (Hardt, 1999; Takemura et al., 2003).

The kinematic model comprises: The cycle time  $T$ , the duty factor  $\beta$ , the transference time  $t_T = (1 - \beta)T$ , the support time  $t_S = \beta T$ , the step length  $L_S$ , the stroke pitch  $S_P$ , the body height  $H_B$ , the maximum foot clearance  $F_C$ , the  $i^{\text{th}}$  leg lengths  $L_{i1}$  and  $L_{i2}$ , the  $i^{\text{th}}$  foot length  $L_{i3}$  and the foot trajectory offset  $O_i$  ( $i = 1, \dots, n$ ). Moreover, we consider a periodic trajectory for each foot, with constant body velocity  $V_F = L_S/T$ . Motion is described by means of a world coordinate system.

Gaits describe sequences of leg movements, alternating between transfer and support phases. Given a particular gait and duty factor  $\beta$ , it is possible to calculate, for leg  $i$ , the corresponding phase  $\phi_i$ , the time instant at which each leg leaves and returns to contact with the ground and the cartesian trajectories of the tip of the feet which must be completed during  $t_T$  (Silva et al., 2005). Based on this data, the trajectory generator is responsible for producing a motion that synchronises and coordinates all legs.

When the robot leg is equipped with a foot (i.e., the robot legs have three DoF), there is the need to consider an additional variable, namely the angle between the foot and the ground (which is assumed to be horizontal)  $\theta_{i3hd}$ . Depending on the planned value of this angle, the robot can walk on its toe tips ( $\theta_{i3hd} < 0$ ), plant the whole foot simultaneously on the ground ( $\theta_{i3hd} = 0$ ) or walk on its heels ( $\theta_{i3hd} > 0$ ).

The robot body (and by consequence the hips) is assumed to be desired to have horizontal movement with a constant forward speed  $V_F$ . However, it is necessary to adjust the height of the body from the ground, depending on the planned value of  $\theta_{i3hd}$ . Therefore, if it is

considered that the robot walks on its toe tips ( $\theta_{i3hd} < 0$ ), for leg  $i$  the cartesian coordinates of the hip of the legs are given by  $\mathbf{p}_{Hd}(t) = [x_{iHd}(t), y_{iHd}(t)]^T$ :

$$\mathbf{p}_{Hd}(t) = [V_F t + Sp(1 - \text{ceil}(i/2)) \quad H_B + L_{i3} \sin(\theta_{i3hd})]^T. \quad (1)$$

The trajectories of the tips of the feet must be arranged in such a way as to avoid collisions with the ground or any obstacles in the vicinity of the robot. This problem is more acute when the robot is walking with a periodic gait because, during locomotion over irregular terrains, where it may be necessary to adopt a non-periodic locomotion gait, it may be necessary to have a distinct trajectory for each individual robot foot. Several different strategies have been proposed for solving this problem (Silva et al., 2005).

Based on the model under consideration, the desired trajectory of the foot for each cycle of the leg swing is computed through a cycloid function (equation (2)) (Silva et al., 2003b). For example, considering that the transfer phase starts at  $t = 0$  s for leg  $i = 1$  we have for  $\mathbf{p}_{Fd}(t) = [x_{iFd}(t), y_{iFd}(t)]^T$ :

During the transfer phase:

$$\mathbf{p}_{Fd}(t) = \begin{bmatrix} V_F \left[ t - \frac{t_T}{2\pi} \sin\left(\frac{2\pi t}{t_T}\right) \right] \\ \frac{F_C}{2} \left[ 1 - \cos\left(\frac{2\pi t}{t_T}\right) \right] \end{bmatrix}. \quad (2)$$

During the stance phase:

$$\mathbf{p}_{Fd}(t) = [V_F T \quad 0]^T. \quad (3)$$

Once the coordinates of the hips and feet of the robot are defined, it is possible to obtain the leg joint positions and velocities using the inverse kinematics  $\boldsymbol{\psi}^{-1}$  and the Jacobian  $\mathbf{J} = \partial\boldsymbol{\psi}/\partial\boldsymbol{\Theta}_d$ .

The algorithm for planning forward motion accepts the desired cartesian trajectories of the legs' hips  $\mathbf{p}_{Hd}(t)$  and feet  $\mathbf{p}_{Fd}(t)$  as inputs and, by means of an inverse kinematics algorithm  $\boldsymbol{\psi}^{-1}$ , generates the related joint trajectories  $\boldsymbol{\Theta}_d(t) = [\theta_{i1d}(t), \theta_{i2d}(t), \theta_{i3d}(t)]^T$ , selecting the solution corresponding to a forward knee and a backward ankle:

$$\mathbf{p}_d(t) = [x_{id}(t) \quad y_{id}(t)]^T = \mathbf{p}_{Fd}(t) - \mathbf{p}_{Hd}(t) \quad (4a)$$

$$\mathbf{p}_d(t) = \boldsymbol{\psi}[\boldsymbol{\Theta}_d(t)] \Rightarrow \boldsymbol{\Theta}_d(t) = \boldsymbol{\psi}^{-1}[\mathbf{p}_d(t)] \quad (4b)$$

$$\dot{\boldsymbol{\Theta}}_d(t) = \mathbf{J}^{-1}[\dot{\mathbf{p}}_d(t)], \quad \mathbf{J} = \frac{\partial\boldsymbol{\psi}}{\partial\boldsymbol{\Theta}_d}. \quad (4c)$$

In order to avoid impact and friction effects, zero velocities of the feet for the instants of landing and taking off are assumed at the planning phase, which also insures velocity continuity.

### 3. ROBOT DYNAMIC MODEL

#### 3.1. Computation of Inverse Dynamics

The planned joint trajectories constitute the reference for the robot control system. The model for the robot inverse dynamics is formulated as:

$$\Gamma = \mathbf{H}(\Theta) \ddot{\Theta} + \mathbf{c}(\Theta, \dot{\Theta}) + \mathbf{g}(\Theta) - \mathbf{F}_{RH} - \mathbf{J}_F^T(\Theta) \mathbf{F}_{RF} \quad (5)$$

where  $\Gamma = [f_{ix}, f_{iy}, \tau_{i1}, \tau_{i2}, \tau_{i3}]^T$  ( $i = 1, \dots, n$ ) is the vector of forces/torques,  $\Theta = [x_{iH}, y_{iH}, \theta_{i1}, \theta_{i2}, \theta_{i3}]^T$  is the vector of position coordinates,  $\mathbf{H}(\Theta)$  is the inertia matrix and  $\mathbf{c}(\Theta, \dot{\Theta})$  and  $\mathbf{g}(\Theta)$  are the vectors of centrifugal/Coriolis and gravitational forces/torques, respectively. The  $n \times m$  ( $m = 3$ ) matrix  $\mathbf{J}_F^T(\Theta)$  is the transpose of the robot Jacobian matrix,  $\mathbf{F}_{RH}$  is the  $m \times 1$  vector of the body inter-segment forces and  $\mathbf{F}_{RF}$  is the  $m \times 1$  vector of the reaction forces that the ground exerts on the robot feet. These forces are zero during the foot transfer phase. During the system simulation, equation (5) is integrated using the Runge-Kutta method. Furthermore, non-ideal joint actuators exhibiting saturation are considered:

$$\tau_{ijm} = \begin{cases} \tau_{ijc} & , \quad |\tau_{ijm}| \leq \tau_{ijMax} \\ \text{sgn}(\tau_{ijc}) \cdot \tau_{ijMax} & , \quad |\tau_{ijm}| > \tau_{ijMax} \end{cases} \quad (6)$$

where, for leg  $i$  and joint  $j$ ,  $\tau_{ijc}$  is the torque demanded by the controller,  $\tau_{ijMax}$  is the maximum torque that the actuator can supply and  $\tau_{ijm}$  is the effective motor torque.

#### 3.2. Joint $j = 3$ Implementation

Bearing in mind the fact that most living animals have compliant feet and ankles, in order to diminish the forces created by impact on the ground and to prevent the occurrence of chattering (in which the foot repeatedly abandons and returns to contact with the ground before the contact stabilizes) (Hardt, 1999; Alexander, 1990), in this work it is considered that joint  $j = 3$  can be either mechanically actuated (i.e., passive) or motor actuated. For the mechanically actuated case, we suppose that there is a rotational spring-dashpot system connecting links  $L_{i2}$  and  $L_{i3}$ . This mechanical impedance maintains the angle between the two links and imposes a joint torque given (for leg  $i$ ) by:

$$\begin{aligned} \tau_{i3m} &= K_3 \Delta_{i3} + B_3 \dot{\Delta}_{i3} \\ \Delta_{i3} &= \theta_{i3d}(t) - \theta_{i3}(t), \quad \dot{\Delta}_{i3} = \dot{\theta}_{i3d}(t) - \dot{\theta}_{i3}(t) \end{aligned} \quad (7)$$

where  $\tau_{i3m}$  is the effective joint torque,  $K_3$  and  $B_3$  are the coefficients of stiffness and viscous friction and  $\theta_{i3d}$  and  $\theta_{i3}$  are the planned and real joint trajectories.

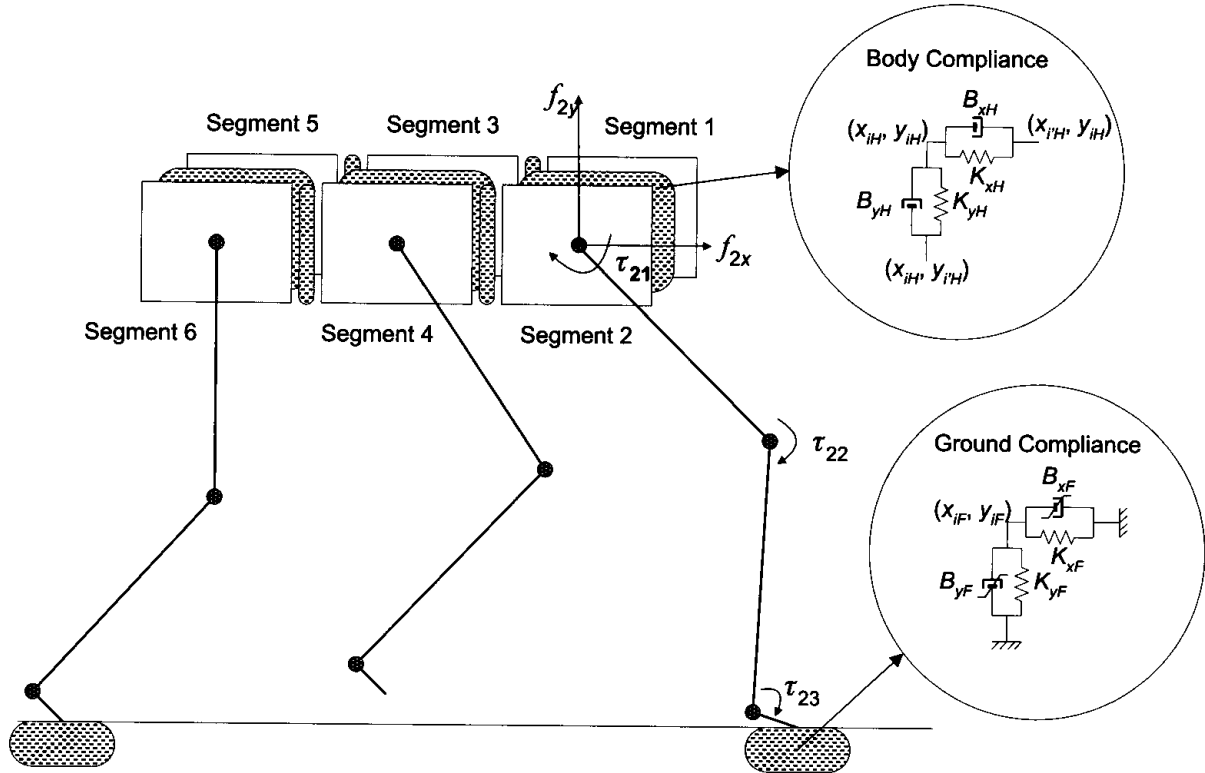


Figure 3. Robot body and foot-ground interaction models.

### 3.3. Robot Body Model

Figure 3 presents the dynamic model for the hexapod body and foot-ground interaction. Robot body compliance is considered because walking animals have a spine that allows improved stability while supporting the locomotion (Witte et al., 2001). This model is inspired by several studies that highlight this structure. For example, the hedgehog possesses muscles in the omoplata that apparently act as spring-dashpot systems. This biomechanical structure absorbs part of the energy generated during the foot's contact with the ground and returns that energy just before the feet lift off the ground (Villanova et al., 2000). Several other authors have also followed this line of thought (see, e.g., Berns et al., 1998; Zhifeng et al., 2003).

The robot body is divided into  $n$  identical segments (each with mass  $M_{bn}^{-1}$ ) and a linear spring-dashpot system is adopted to implement the intra-body compliance:

$$f_{ixH} = \sum_{i'=1}^u [-K_{xH} (x_{iH} - x_{i'H}) - B_{xH} (\dot{x}_{iH} - \dot{x}_{i'H})] \quad (8a)$$

$$f_{iyH} = \sum_{i'=1}^u [-K_{yH} (y_{iH} - y_{i'H}) - B_{yH} (\dot{y}_{iH} - \dot{y}_{i'H})] \quad (8b)$$

where  $(x_{i'H}, y_{i'H})$  are the hip coordinates and  $u$  is the total number of segments adjacent to leg  $i$ .

Table 1. System parameters.

Robot model parameters		Locomotion parameters	
$S_p$	1 m	$\beta$	50%
$L_{ij}, j = 1, 2$	0.5 m	$L_S$	1 m
$L_{i3}$	0.1 m	$H_B$	0.9 m
$O_i$	0 m	$F_C$	0.1 m
$M_b$	88.0 kg	$V_F$	1 ms <sup>1</sup>
$M_{ij}, j = 1, 2$	1 kg	Ground parameters	
$M_{i3}$	0.1 kg	$K_{xF}$	$1.3 \times 10^6 \text{ Nm}^{-1}$
$K_{xH}$	$10^5 \text{ Nm}^{-1}$	$K_{yF}$	$1.7 \times 10^6 \text{ Nm}^{-1}$
$K_{yH}$	$10^4 \text{ Nm}^{-1}$	$B_{xF}$	$2.3 \times 10^6 \text{ Nsm}^{-1}$
$B_{xH}$	$10^3 \text{ Nsm}^{-1}$	$B_{yF}$	$2.7 \times 10^6 \text{ Nsm}^{-1}$
$B_{yH}$	$10^2 \text{ Nsm}^{-1}$	$\nu$	0.9

Different methods have been proposed (Villanova et al., 2000; Bhat, 2003) for the definition of the numerical values for the parameters of equations (8a) and (8b). The parameters  $K_{\eta H}$  and  $B_{\eta H}$  ( $\eta = \{x, y\}$  for the {horizontal, vertical} directions, respectively) are defined so that the body behaviour is similar to that expected in an animal (Table 1).

### 3.4. Foot-Ground Interaction Model

The contact of the  $i^{\text{th}}$  robot foot with the ground is modelled using a non-linear system (Silva et al., 2005) with stiffness  $K_{\eta F}$  and damping  $B_{\eta F}$  ( $\eta = \{x, y\}$ ) (Figure 3), yielding:

$$f_{ixF} = -K_{xF}(x_{iF} - x_{iF0}) - B_{xF}[-(y_{iF} - y_{iF0})](\dot{x}_{iF} - \dot{x}_{iF0}) \quad (9a)$$

$$f_{iyF} = -K_{yF}(y_{iF} - y_{iF0}) - B_{yF}[-(y_{iF} - y_{iF0})]^{\nu}(\dot{y}_{iF} - \dot{y}_{iF0}) \quad (9b)$$

where  $x_{iF0}$  and  $y_{iF0}$  are the coordinates of touchdown for foot  $i$ , and  $\nu \approx 1.0$  is a parameter dependent on the ground characteristics. The values for the parameters  $K_{\eta F}$  and  $B_{\eta F}$  (Table 1) are based on studies of soil mechanics (Silva et al., 2003b; Silva et al., 2005).

## 4. CONTROL ARCHITECTURE

The general control architecture of the hexapod robot is presented in Figure 4. Trajectory planning is carried out in the cartesian space, but control is performed in the joint space, which requires the integration of the inverse kinematic model in the forward path. The base algorithm considers only position feedback and, in that case, the series of  $G_{c1}(s)$  and  $G_{c2}$  can be replaced by a single block. Nevertheless, the base architecture is improved by the introduction of a second internal feedback loop with information about the foot-ground interaction force. In the case of force feedback,  $G_{c1}(s)$  and  $G_{c2}$  form a cascade structure in the forward control path.

In a previous work, the advantages of this controller structure (i.e., PD position control and foot force feedback) over the base structure (having only position feedback) were

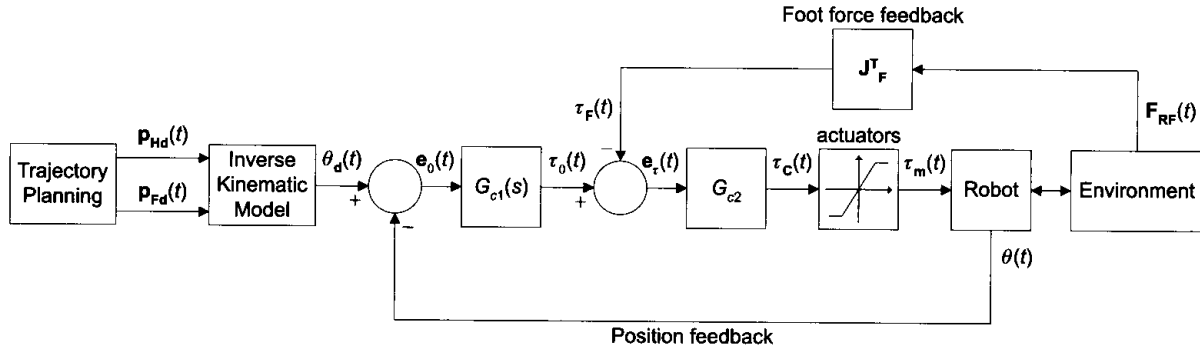


Figure 4. Hexapod robot control architecture.

demonstrated for the case of joint control of hexapod robots having legs with two DoF. The improved performance after the introduction of force feedback was particularly notable for the cases of non-ideal actuators with saturation or variable ground characteristics (Silva et al., 2003b).

Fractional order controllers often achieve better performance and robustness results when compared with integer order ones, particularly when the system under control presents fractional dynamics, as seems to be the case here (Silva et al., 2006a).

Based on these results, in this study we evaluate the effect of different FO PD<sup>α</sup> controller implementations for  $G_{c1}(s)$ . For  $G_{c2}$  a simple  $P$  controller with gain  $Kp_j = 0.9$  ( $j = 1, 2, 3$ ) is used; the use of a PD algorithm in  $G_{c2}$  would introduce noise over the foot force feedback signal while the adoption of a PI controller would tend to make this inner loop unstable. For the FO PD<sup>α</sup> algorithm we have, for joint  $j$ :

$$G_{C1j}(s) = Kp_j + K\alpha_j s^{\alpha_j}, \quad \alpha_j \in \mathfrak{R}, \quad j = 1, 2, 3 \tag{10}$$

where  $Kp_j$  and  $K\alpha_j$  are the proportional and derivative gains, respectively, and  $\alpha_j \in \mathfrak{R}$  is the fractional order. Therefore, the classical PD<sup>1</sup> algorithm occurs when the fractional order  $\alpha_j = 1.0$ . The FO PD<sup>α</sup> algorithm can be seen as a generalisation of the integer order PD (Figure 5).

In the context of equation (10), it should be noted that the mathematical definition of a derivative of fractional order has been the subject of several different approaches (Machado, 1997). For example, equations (11a) and (11b) represent the Laplace (for zero initial conditions) and Grünwald-Letnikov definitions of the fractional derivative of order  $\alpha$  of the signal  $x(t)$ :

$$D^\alpha[x(t)] = L^{-1}\{s^\alpha X(s)\} \tag{11a}$$

$$D^\alpha[x(t)] = \lim_{h \rightarrow 0} \left[ \frac{1}{h^\alpha} \sum_{k=1}^{\infty} \frac{(-1)^k \Gamma(\alpha + 1)}{\Gamma(k + 1) \Gamma(\alpha - k + 1)} x(t - kh) \right] \tag{11b}$$

where  $\Gamma$  is the gamma function and  $h$  is the time increment.

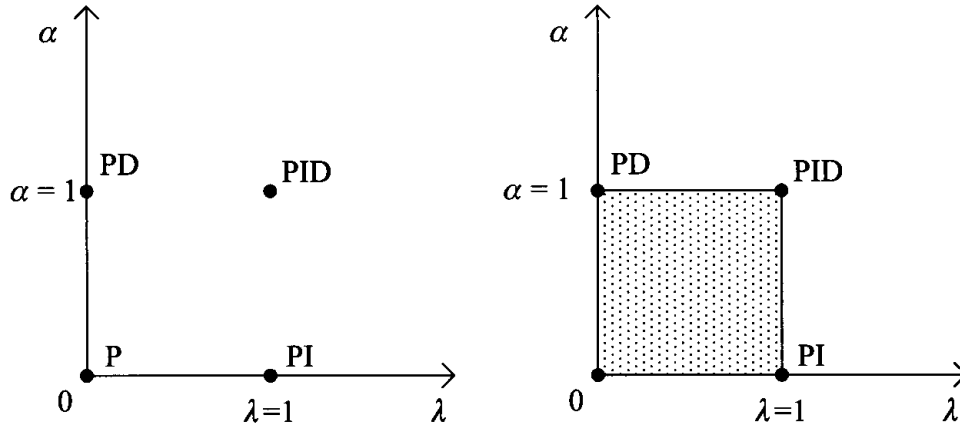


Figure 5. Generalisation of a PID controller: Classical integer order PID “family” of controllers (left) and fractional order PID (PI<sup>λ</sup>D<sup>α</sup>) (Podlubny et al., 1997) (right).

The FO algorithm (equation (10)) was implemented using a discrete-time 4<sup>th</sup> order Padé approximation ( $a_{ij}, b_{ij} \in \mathfrak{R}, j = 1, 2, 3$ ) (Silva et al., 2006b), yielding an equation in the  $z$ -domain of the type (Barbosa et al., 2006):

$$G_{C1j}(z) \approx Kp_j + K\alpha_j \frac{\sum_{i=0}^{i=4} a_{ij} z^{-i}}{\sum_{i=0}^{i=4} b_{ij} z^{-i}} \quad (12)$$

where  $Kp_j$  and  $K\alpha_j$  are the proportional and derivative gains, respectively.

## 5. MEASURES FOR PERFORMANCE EVALUATION

In mathematical terms we will now establish two global measures of the mechanism’s overall (average) locomotion performance. We define one index  $\{E_{av}\}$  based on the system dynamics and the other  $\{\varepsilon_{xyH}\}$  based on the trajectory tracking errors.

The first measure is the mean absolute density of energy per travelled distance  $E_{av}$ . This index is computed assuming that energy regeneration is not available for actuators doing negative work; that is, by taking the absolute value of the power. At a given joint  $j$  (each leg has  $m = 3$  joints) and leg  $i$  (since we are designing a hexapod,  $n = 6$  legs), the mechanical power is the product of the motor torque and angular velocity. The global index  $E_{av}$  is obtained by averaging the absolute mechanical energy delivered over the travelled distance  $d$ :

$$E_{av} = \frac{1}{d} \sum_{i=1}^n \sum_{j=1}^m \int_0^T |\tau_{ij}(t) \dot{\theta}_{ij}(t)| dt \quad [\text{Jm}^{-1}]. \quad (13)$$

We can define the index for the hip trajectory tracking errors as

$$\begin{aligned}\varepsilon_{xyH} &= \sum_{i=1}^n \sqrt{\frac{1}{N_s} \sum_{k=1}^{N_s} (\Delta_{ixH}^2 + \Delta_{iyH}^2)} \quad [\text{m}] \\ \Delta_{ixH} &= x_{iHd}(k) - x_{iH}(k), \Delta_{iyH} = y_{iHd}(k) - y_{iH}(k)\end{aligned}\quad (14)$$

where  $N_s$  is the total number of samples for averaging purposes and  $\{d, r\}$  indicate the  $i^{\text{th}}$  samples of the desired and real position, respectively.

In both cases performance optimization entails the minimization of each index.

## 6. SIMULATION RESULTS

In this section we develop a set of simulations to analyse the performance of the different FO PD $^\alpha$  controller implementations during a periodic wave gait at a constant forward velocity  $V_F$ .

These experiments show the influence of the different controller tunings on the robot's locomotion performance and the trajectories of the hips and feet. The system performance is analyzed for two distinct situations: With two leg joints motor actuated and the ankle joint actuated through a passive mechanical system, and with all three leg joints motor actuated. The simulation results show the superior performance of the FO PD $^\alpha$  controller for a fractional order  $\alpha_j = 0.5$ , when all leg joints are motor actuated.

For simulation purposes we used the parameters given in Table 1 for the locomotion, the robot body and the ground (assuming that the robot is walking on a level surface of compact clay). The discrete-time control algorithm is evaluated with a sampling frequency of  $f_{sc} = 10.0$  kHz while the robot and environment are simulated with a sampling frequency of  $f_{sr} = 100.0$  kHz.

### 6.1. Controller Tuning Methodology

To tune the different controller implementations a systematic method was adopted, testing and evaluating a narrow grid of possible combinations of parameters for all controller implementations. Therefore, we adopt the  $G_{c1}(s)$  parameters that establish a compromise in the context of the simultaneous minimization of  $E_{av}$  and  $\varepsilon_{xyH}$ , and a proportional controller  $G_{c2}$  with gain  $Kp_j = 0.9$  ( $j = 1, 2, 3$ ).

Moreover, high performance joint actuators are assumed, with a maximum actuator torque in equation (6) of  $\tau_{ijMax} = 400$  Nm and  $\theta_{i3hd} = -\pi/12$  rad (Silva, *et al.*, 2006c).

We start by considering the case where leg joints 1 and 2 are motor actuated and joint 3 is mechanically actuated. For this case we tune the FO PD $^\alpha$  joint controllers for different values of the fractional order  $\alpha_j$  in the interval  $-0.9 \leq \alpha_j \leq +0.9$  and  $\alpha_j \neq 0.0$ . Afterwards, we repeat the controller tuning procedure for the case where all three joints are motor actuated. The controller parameters, for both cases, are presented in Table 2 and the corresponding values of  $E_{av}$  and  $\varepsilon_{xyH}$  are presented in Table 3.

Table 2. Controller parameters.

Fractional order	Joint 3 mechanically actuated		Joint 3 motor actuated	
$\alpha_j = 0.4$	$Kp_1$	10000.0	$Kp_1$	8000.0
	$K\alpha_1$	3200.0	$K\alpha_1$	2900.0
	$Kp_2$	800.0	$Kp_2$	900.0
	$K\alpha_2$	300.0	$K\alpha_2$	400.0
	$K_3$	2.0	$Kp_3$	100.0
	$B_3$	0.5	$K\alpha_3$	80.0
$\alpha_j = 0.5$	$Kp_1$	15000.0	$Kp_1$	15000.0
	$K\alpha_1$	6000.0	$K\alpha_1$	7200.0
	$Kp_2$	1000.0	$Kp_2$	1000.0
	$K\alpha_2$	600.0	$K\alpha_2$	800.0
	$K_3$	0.5	$Kp_3$	150.0
	$B_3$	2.0	$K\alpha_3$	240.0
$\alpha_j = 0.6$	$Kp_1$	2500.0	$Kp_1$	600.0
	$K\alpha_1$	800.0	$K\alpha_1$	150.0
	$Kp_2$	300.0	$Kp_2$	250.0
	$K\alpha_2$	100.0	$K\alpha_2$	40.0
	$K_3$	1.0	$Kp_3$	100.0
	$B_3$	2.0	$K\alpha_3$	15.0
$\alpha_j = 0.7$	$Kp_1$	2000.0	$Kp_1$	600.0
	$K\alpha_1$	500.0	$K\alpha_1$	150.0
	$Kp_2$	400.0	$Kp_2$	150.0
	$K\alpha_2$	100.0	$K\alpha_2$	15.0
	$K_3$	0.5	$Kp_3$	80.0
	$B_3$	0.5	$K\alpha_3$	15.0
$\alpha_j = 0.8$	$Kp_1$	2000.0	$Kp_1$	500.0
	$K\alpha_1$	400.0	$K\alpha_1$	80.0
	$Kp_2$	300.0	$Kp_2$	200.0
	$K\alpha_2$	100.0	$K\alpha_2$	30.0
	$K_3$	4.0	$Kp_3$	80.0
	$B_3$	3.5	$K\alpha_3$	10.0

 Table 3. Values of  $E_{av}$  and  $\varepsilon_{xyH}$  corresponding to the best controller tuning for different values of  $\alpha_j$  when joint 3 is mechanically actuated and motor actuated.

Fractional order $\alpha_j$	Joint 3 mechanically actuated		Joint 3 motor actuated	
	$E_{av}$ [ $\text{Jm}^{-1}$ ]	$\varepsilon_{xyH}$ [m]	$E_{av}$ [ $\text{Jm}^{-1}$ ]	$\varepsilon_{xyH}$ [m]
0.4	724.5	1.99	629.3	2.60
0.5	564.2	1.93	367.6	0.97
0.6	490.1	1.91	465.0	1.58
0.7	5279.2	1.95	432.7	1.06
0.8	10379.1	2.33	479.7	0.78

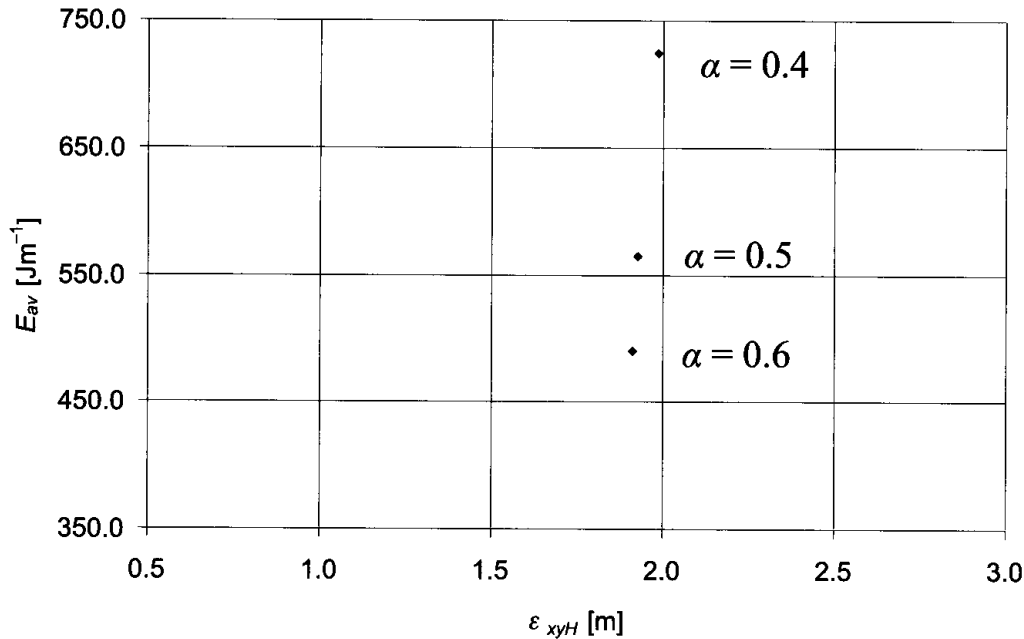


Figure 6. Performance indices  $E_{av}$  vs.  $\varepsilon_{xyH}$  for different  $G_{c1}(s)$  FO PD $^\alpha$  controller tunings, when establishing a compromise between the minimization of  $E_{av}$  and  $\varepsilon_{xyH}$ , with  $G_{c2} = 0.9$ , joints 1 and 2 motor actuated and joint 3 mechanically actuated.

## 6.2. FO PD $^\alpha$ Algorithm Performance

Figure 6 presents the optimum controller tuning for different values of  $\alpha_j$  when joint 3 is mechanically actuated.

We observe that the value  $\alpha_j = 0.6$  presents the best compromise situation for the simultaneous minimization of  $\varepsilon_{xyH}$  and  $E_{av}$ . The values of  $\varepsilon_{xyH}$  for  $\alpha_j = \{0.4, 0.5, 0.7\}$  are slightly higher than for  $\alpha_j = 0.6$ . For  $\alpha_j = 0.8$  the index  $\varepsilon_{xyH}$  yields much higher values. The minimum value of  $E_{av}$  is obtained for  $\alpha_j = 0.6$ , increasing for  $\alpha_j = 0.5$  and  $\alpha_j = 0.4$ . For  $\alpha_j = \{0.7, 0.8\}$  the values of  $E_{av}$  are much higher, and are not presented in Figure 6.

Figure 7 shows a similar chart for the case where all joints are motor actuated. Here,  $\alpha_j = 0.5$  presents the best compromise situation for the simultaneous minimization of  $\varepsilon_{xyH}$  and  $E_{av}$ ; the values of  $\varepsilon_{xyH}$  and  $E_{av}$  are slightly higher for  $\alpha_j = \{0.6, 0.7\}$ , while for  $\alpha_j = 0.4$  both  $\varepsilon_{xyH}$  and  $E_{av}$  present much higher values. For  $\alpha_j = 0.8$  the robot locomotion has a lower value of  $\varepsilon_{xyH}$  but a higher value of  $E_{av}$ .

In both cases under consideration for the actuation of joint 3, the results for  $\alpha_j = \{0.1, 0.2, 0.3\}$  are very poor. Moreover, for  $-0.9 < \alpha_j < -0.1$  and for  $\alpha_j = 0.9$  the hexapod locomotion is unstable.

Comparing Figures 6 and 7 we conclude that, for the same fractional order, the best result occurs when all leg joints are motor actuated. This can also be seen in Figures 8 and 9, which present the joint actuation torques  $\tau_{1jm}(t)$  and the hip trajectory tracking errors  $\Delta_{1xH}(t)$  and  $\Delta_{1yH}(t)$  for the two cases (ankle joint mechanically actuated and motor actuated), for the controller fractional order  $\alpha_j = 0.5$ . Moreover, when joint 3 is mechanically actuated, the curves of the joint torques show larger oscillations than when it is motor actuated. This is due to the fact that there is some oscillation of joint three during the support phase.

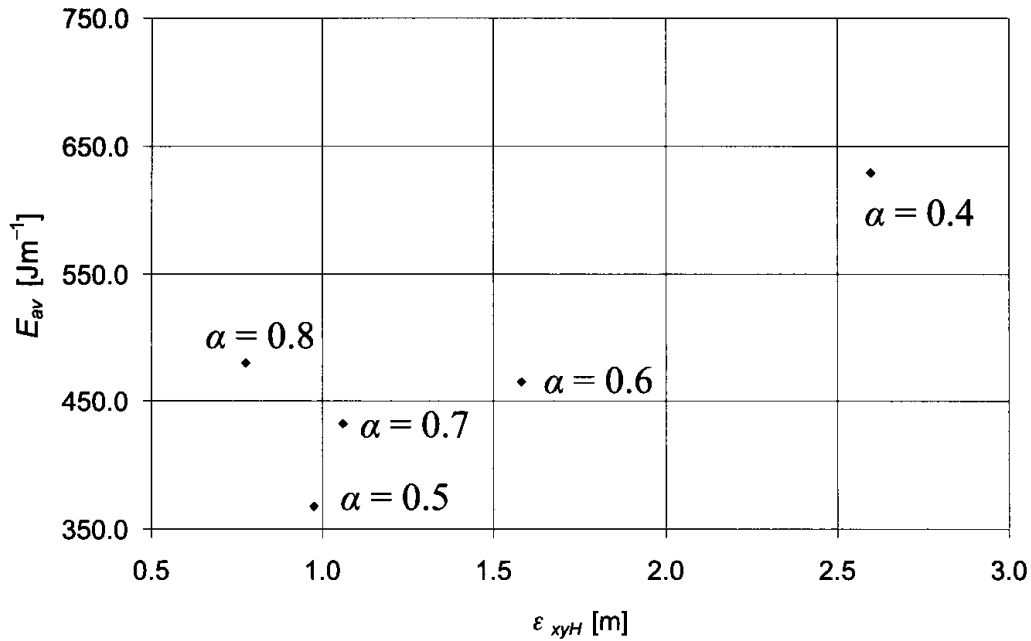


Figure 7. Performance indices  $E_{av}$  vs.  $\varepsilon_{xyH}$  for different  $G_{c1}(s)$  FO PD<sup>α</sup> controller tunings, when establishing a compromise between the minimization of  $E_{av}$  and  $\varepsilon_{xyH}$ , with  $G_{c2} = 0.9$  and all joints motor actuated.

It is worth mentioning that when joint 3 is mechanically actuated, the robot puts the toe tips onto the ground, followed by the heel. Both remain in this state during the foot's support phase and, consequently, the robot walks supporting its body over link  $L_{i3}$ . When all joints are motor actuated, however, the robot walks on its toe tips during the feet support phase (i.e., the hexapod supports itself on the extremity of link  $L_{i3}$ ).

From the biological point of view both cases are important. Therefore, further study is necessary to investigate more deeply how the behaviour changes with the locomotion parameters.

### 6.3. Ground Properties

Since the objective of walking robots is to be able to walk over natural terrains, we next examined how the different FO PD<sup>α</sup> joint leg controllers behave for different ground properties, for both joint 3 actuation alternatives. The values of  $\{K_{xF}, B_{xF}, K_{yF}$  and  $B_{yF}\}$  were varied simultaneously through a multiplying factor  $K_{mult}$  that was varied over the range 0.1 to 4.0, for both joint 3 actuation types, using the previously discussed values of the controller parameters. This variation of the ground model parameters allows the simulation of ground behaving with increasing stiffness, from peat to gravel (Silva et al., 2003b).

The performance measures are presented against the multiplying factor of the ground parameters  $K_{mult}$  in Figures 10 and 11, for the cases of joint 3 being mechanically actuated and motor actuated, respectively. We conclude that the controller responses are quite similar, meaning that these algorithms are robust to variations of the ground characteristics.

Based on Figure 10 it is possible to conclude that, to minimize  $E_{av}$ , the best FO PD<sup>α</sup> controller implementation occurs for the fractional order  $\alpha_j = 0.6$ , followed by  $\alpha_j = 0.5$

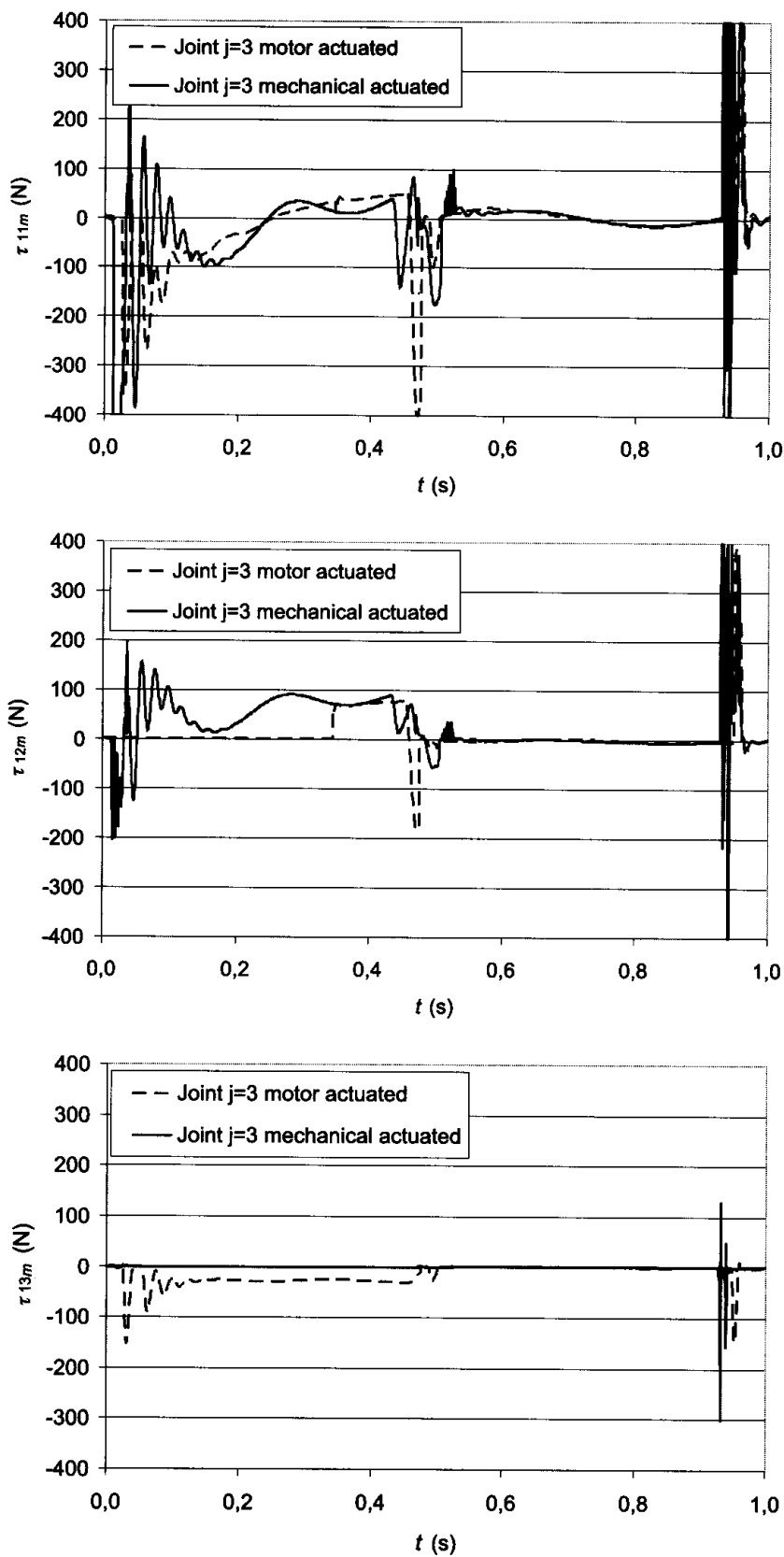


Figure 8. Time evolution of  $\tau_{1jm}$ , with joints 1 and 2 motor actuated and joint 3 mechanically actuated, and with all joints motor actuated ( $\alpha_j = 0.5$ ).

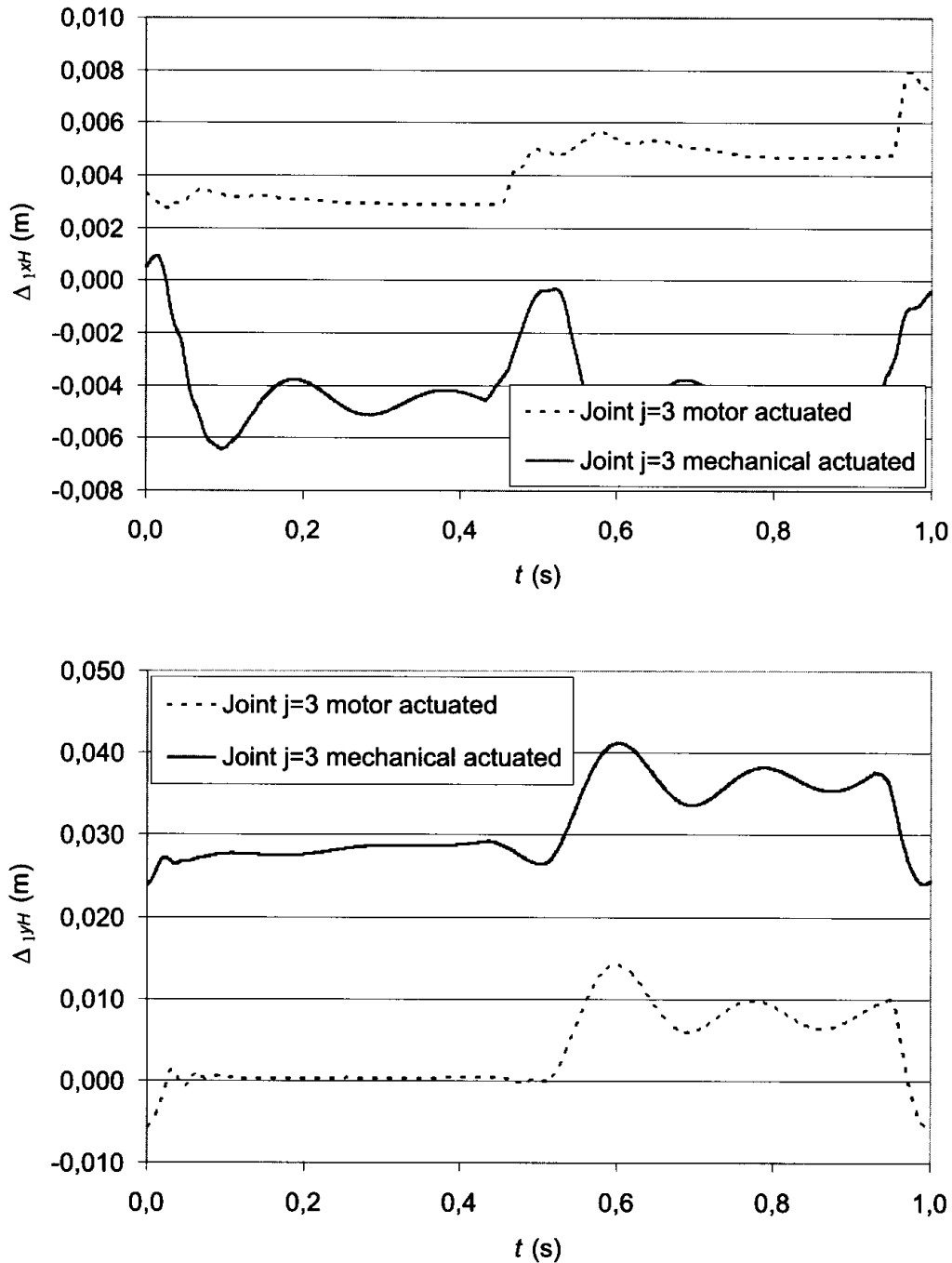


Figure 9. Time evolution of  $\Delta_{1xH}$  and  $\Delta_{1yH}$ , with joints 1 and 2 motor actuated and joint 3 mechanically actuated, and with all joints motor actuated ( $\alpha_j = 0.5$ ).

and  $\alpha_j = 0.4$ . Moreover, it is clear that the performances of the different controller implementations are almost constant over the whole range of variation of the ground parameters.

For  $\varepsilon_{xyH}$  (Figure 10) it is clear that the controller implementations corresponding to the fractional orders  $\alpha_j = \{0.5, 0.6, 0.7\}$  present the lower values for all values of  $K_{mult}$ . The fractional orders  $\alpha_j = \{0.4, 0.8\}$  lead to controller implementations with inferior performance in this regard, particularly for hard soils ( $K_{mult} > 2.0$ ). It is also noticeable that for soft soils ( $K_{mult} < 0.5$ ) most of the controllers reveal a degraded performance.

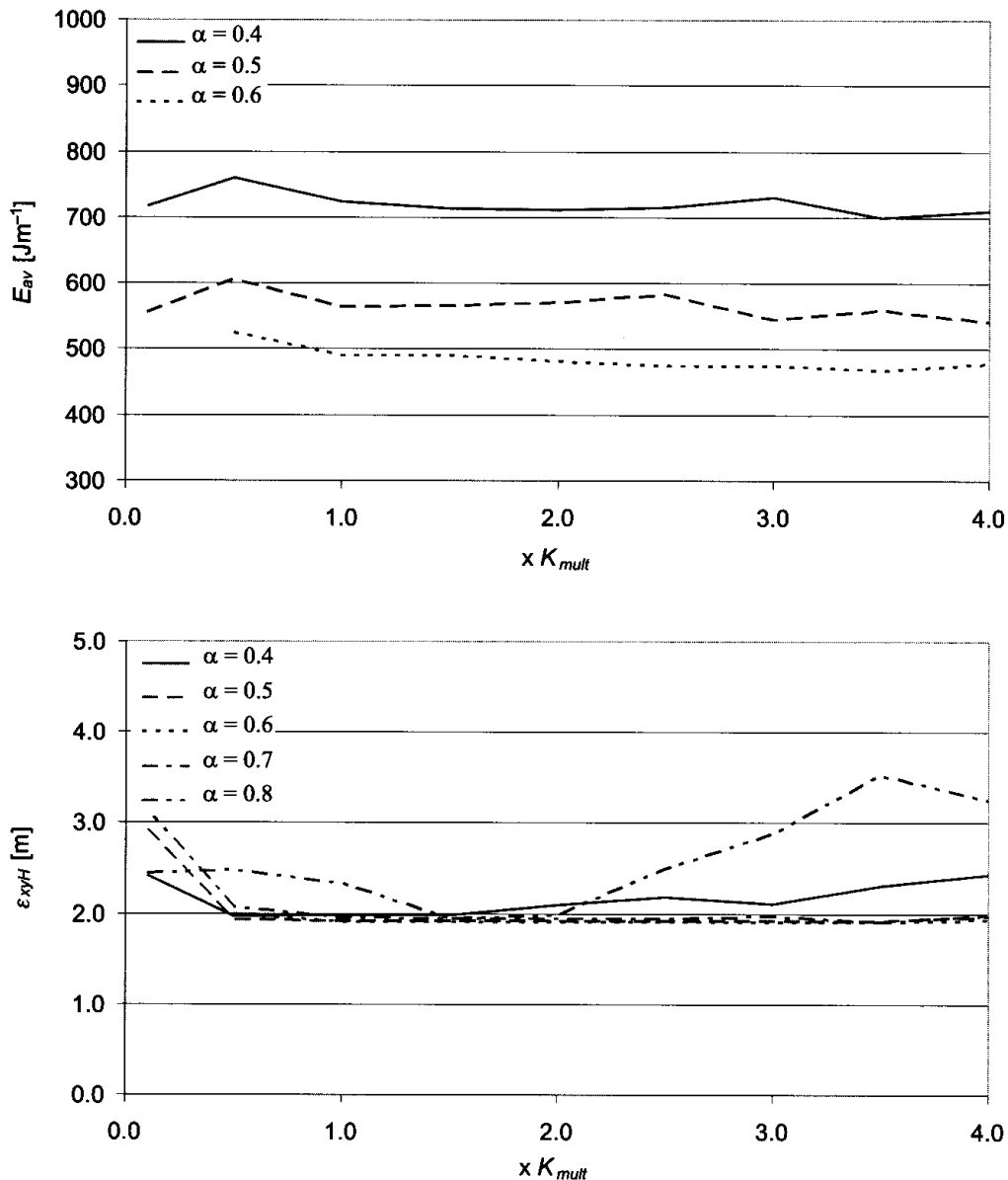


Figure 10. Performance indices  $E_{av}$  and  $\epsilon_{xyH}$  vs.  $K_{mult}$  for different  $G_{c1}(s)$  FO PD $^\alpha$  controller tunings with joints 1 and 2 motor actuated and joint 3 mechanically actuated.

For the case where joint 3 is motor actuated, and analysing the system's performance from the viewpoint of minimizing  $E_{av}$  (Figure 11), it is possible to conclude that the best FO PD $^\alpha$  implementation occurs for the fractional order  $\alpha_j = 0.5$ . Again, it is clear that the performances of the different controller implementations are almost constant over the whole range of the ground parameters, with the exception of the fractional order  $\alpha_j = 0.4$ , where  $E_{av}$  undergoes significant variation with  $K_{mult}$ .

When the system performance is evaluated in terms of minimizing  $\epsilon_{xyH}$  (Figure 11), we can see that the controller implementations corresponding to the fractional orders  $\alpha_j = \{0.6, 0.7, 0.8\}$  present the best values. The fractional order  $\alpha_j = 0.5$  leads to controller implementations with a slightly inferior performance, particularly for values of  $K_{mult} > 2.5$ .

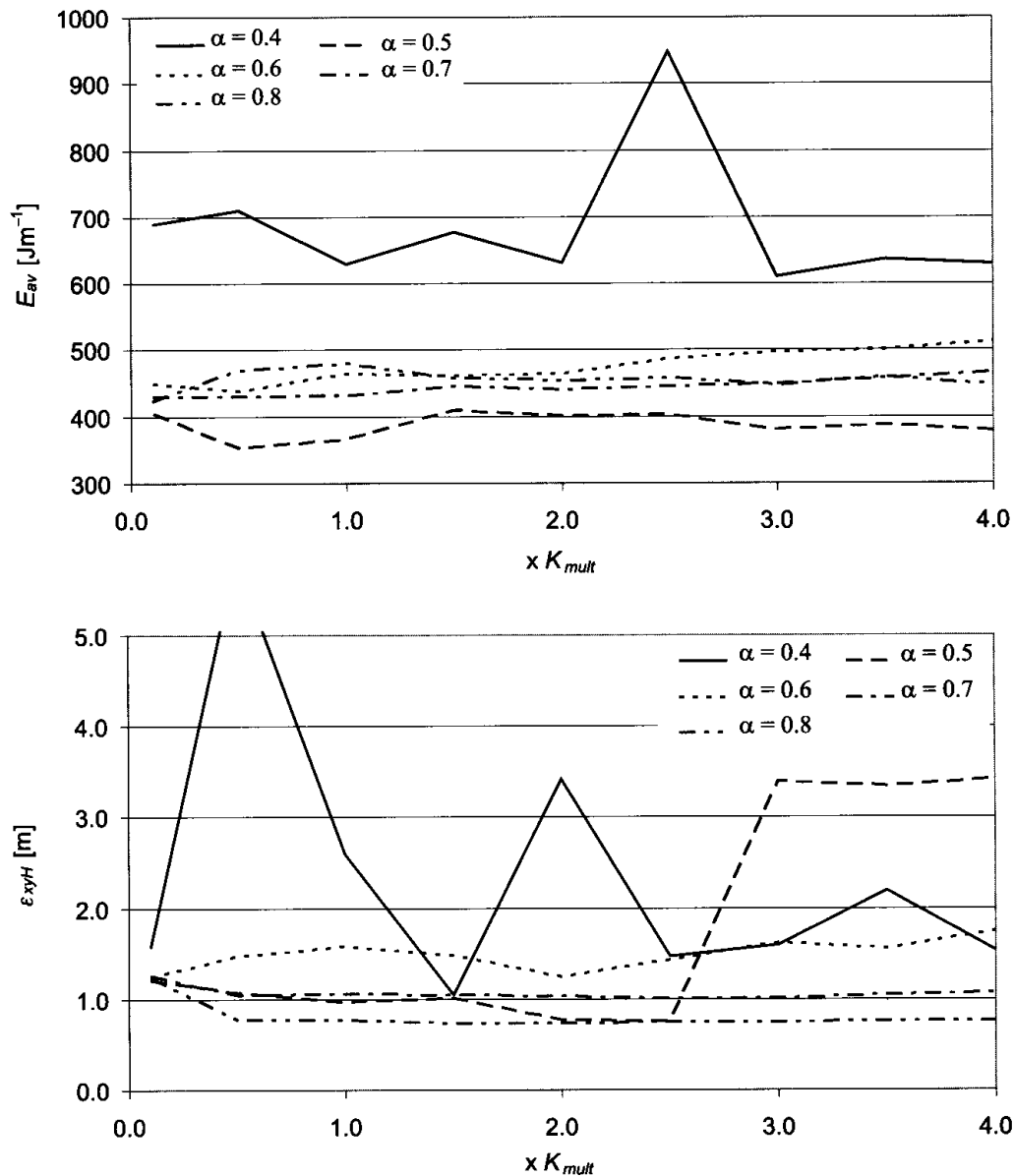


Figure 11. Performance indices  $E_{av}$  and  $\varepsilon_{xyH}$  vs.  $K_{mult}$  for different  $G_{c1}(s)$  FO PD<sup>α</sup> controller tunings with all joints motor actuated.

It is also clear on the chart of  $\varepsilon_{xyH}$  vs.  $K_{mult}$  that the fractional order  $\alpha_j = 0.4$  produces a controller implementation with a poor performance.

Comparing Figures 10 and 11, we conclude that the best case corresponds to all the robot leg joints being motor actuated. Moreover, the controllers with  $\alpha_j = \{0.5, 0.6, 0.7, 0.8\}$  present lower values of the indices  $E_{av}$  and  $\varepsilon_{xyH}$  for almost all the values of  $K_{mult}$  under consideration. The only exception to this observation occurs for the FO PD<sup>α</sup> controller implementation when  $\alpha_j = 0.5$ , which presents slightly higher values of the index  $\varepsilon_{xyH}$  for values of  $K_{mult} > 2.5$  when all robot leg joints are motor actuated that when the third joint is mechanically actuated.

## 7. CONCLUSIONS

In this paper we have compared the performance of different FO PD<sup>α</sup> algorithms for leg joint control of a hexapod robot, both for systems having a passive mechanical ankle, and robots with a motor actuated ankle joint.

In order to analyze the system performance two measures were defined, based on the mean absolute density of energy per travelled distance and the hip trajectory errors. The experiments reveal the superior performance of the FO controller for  $\alpha_j \approx 0.5$  and a robot with all joints motor actuated. The superior performance of the FO PD<sup>α</sup> joint leg controller, for the fractional order  $\alpha_j \approx 0.5$ , is retained for a variety of ground properties.

The focus of the presented work has been on controllers with a proportional plus a fractional-order derivative term. A subject that deserves future study is the applicability of a FO PID control algorithm of the type PI<sup>λ</sup>D<sup>α</sup> to this artificial locomotion system and the analysis of the system performance. Another topic that also deserves attention is the effect of introducing a fractional order controller in the  $G_{c2}$  control block. Future work in this area will also address the study of the action of these controllers when the robot is required to walk over other distinct ground conditions, in the presence of obstacles and when considering different locomotion parameters.

## REFERENCES

- Alexander, R. McN., 1990, "Three uses for springs in legged locomotion," *International Journal of Robotics Research* **9**(2), 53–61.
- Alexander, R. McN., 1995, "How animals move," Mavis Multimedia, Mavis Technologies Ltd. (in CD-ROM).
- Barbosa, R. S., Machado, J. A. T., and Silva, M. F., 2006, "Time domain design of fractional differintegrators using least-squares approximations," *Signal Processing* **80**(10), 2567–2581. (already published).
- Berns, K., Ilg, W., Deck, M., and Dillmann, R., 1998, "The mammalian-like quadrupedal walking machine BISAM," in *Proceedings of the 5<sup>th</sup> International Workshop on Advanced Motion Control*, Coimbra, Portugal, pp. 429–433.
- Bhat, R. B., 2003, "Dynamic response of whole body system subjected to walking generated excitation," in *Proceedings of the ASME 19<sup>th</sup> Biennial Conference on Mechanical Vibration and Noise (VIB 2003)*, Chicago, IL, on CD-ROM.
- Celaya, E. and Porta, J., 1995, "Force-based control of a six-legged robot on abrupt terrain using the subsumption architecture," in *Proceedings of the International Conference on Advanced Robotics*, Sant Feliu de Guixols, Catalonia, Spain, pp. 413–419.
- Collins, J. J. and Richmond, S. A., 1994, "Hard-wired central pattern generators for quadrupedal locomotion," *Biological Cybernetics* **71**(5), 375–385.
- Ferrell, C., 1995, "A comparison of three insect inspired locomotion controllers," *Robotics and Autonomous Systems* **16**(2–4), 135–159.
- Hardt, M., 1999, "Multibody dynamical algorithms, numerical optimal control, with detailed studies in the control of jet engine compressors and biped walking," PhD. Thesis, Electrical Engineering, UCSD, La Jolla, CA.
- Lee, K.-P., Koo, T.-W., and Yoon, Y.-S., 1998, "Real-time dynamic simulation of quadruped using modified velocity transformation," in *Proceedings of the IEEE International Conference on Robotics and Automation*, Leuven, Belgium, pp. 1701–1706.
- Machado, J. A. T., 1997, "Analysis and design of fractional-order digital control systems," *Systems Analysis Modeling Simulation* **27**(2–3), 107–122.
- Martins-Filho, L. de S., Silvino, J. L., Resende, P., and Assunção, T. C., 2003, "Control of robotic leg joints – comparing pd and sliding mode approaches," in *Proceedings of the 6<sup>th</sup> International Conference on Climbing and Walking Robots (CLAWAR 2003)*, Catania, Italy, pp. 147–153.

- McGeer, T., 1990, "Passive dynamic walking," *International Journal of Robotics Research* **9**(2), 62–82.
- Podlubny, I., Dorcak, L., and Kostial, I., 1997, "On fractional derivatives, fractional-order dynamic systems and PI<sup>λ</sup>D<sup>μ</sup>-controllers," in *Proceedings of the 36th IEEE Conference on Decision and Control*, San Diego, CA, pp. 4985–4990.
- Silva, M. F., Machado, J. A. T., and Barbosa, R. S., 2006a, "Complex-order dynamics in hexapod locomotion," *Signal Processing* **80**(10), 2785–2793. (in press).
- Silva, M. F., Machado, J. A. T., and Barbosa, R. S., 2006b, "Comparison of different FO PD<sup>α</sup> control algorithm implementations for legged robots," in *Proceedings of the 9th International Conference on Climbing and Walking Robots and the Support Technologies for Mobile Machines (CLAWAR 2006)*, Brussels, Belgium.
- Silva, M. F., Machado, J. A. T., and Jesus, I. S., 2006c, "Modelling and simulation of walking robots with 3 dof legs," in *Proceedings of the 25th IASTED International Conference on Modelling, Identification and Control (MIC 2006)*, Lanzarote, Canary Islands, Spain, pp. 271–276.
- Silva, M. F., Machado, J. A. T., and Lopes, A. M., 2003a, "Comparison of fractional and integer order control of an hexapod robot," in *Proceedings of the ASME 19<sup>th</sup> Biennial Conference on Mechanical Vibration and Noise (VIB 2003)*, Chicago, IL, on CD-ROM.
- Silva, M. F., Machado, J. A. T., and Lopes, A. M., 2003b, "Position/force control of a walking robot," *Machine Intelligence and Robotic Control* **5**(2), 33–44.
- Silva, M. F., Machado, J. A. T., and Lopes, A. M., 2005, "Modelling and simulation of artificial locomotion systems," *Robotica* **23**(5), 595–606.
- Smith, A. C. and Berkemeier, M. D., 1997, "Passive dynamic quadrupedal walking," in *Proceedings of the IEEE International Conference on Robotics and Automation*, Albuquerque, NM, pp. 34–39.
- Song, J., Low, K. H., and Guo, W., 1999, "A simplified hybrid force/position controller method for the walking robots," *Robotica* **17**(6), 583–589.
- Takemura, H., Khiat, A., Iwama, H., Ueda, J., Matsumoto, Y., and Ogasawara, T., 2003, "Study of the toes role in human walk by toe elimination and pressure measurement system," in *Proceedings of the 2003 IEEE International Conference on Systems, Man and Cybernetics*, Washington, DC, pp. 2569–2574.
- Tsai, C.-R. and Lee, T.-T., 1998, "A study of fuzzy-neural force control for a quadrupedal walking machine," *Journal of Dynamic Systems, Measurement and Control* **120**(1), 124–133.
- Tsai, C.-R., Lee, T.-T., and Song, S.-M., 1997, "Fuzzy logic control of a planetary gear type walking machine leg," *Robotica* **15**(5), 533–546.
- Villanova, J., Guinot, J.-C., Neveu, P., and Gasc, J.-P., 2000, "Quadrupedal mammal locomotion dynamics 2D model," in *Proceedings of the IEEE/RSJ International Conference on Intelligent Robotics and Systems*, Takamatsu, Japan, pp. 1785–1790.
- Witte, H., Hackert, R., Fischer, M. S., Ilg, W., Albiez, J., Dillmann, R., and Seyfarth, A., 2001, "Design criteria for the leg of a walking machine derived by biological inspiration from quadrupedal mammals," in *Proceedings of the 4th International Conference on Climbing and Walking Robots (CLAWAR 2001)*, Karlsruhe, Germany, pp. 63–68.
- Zhifeng, C., Xiuli, Z., Haojun, Z., and Liyao, Z., 2003, "The CPG-based bionic quadruped system," in *Proceedings of the IEEE International Conference on Systems, Man and Cybernetics*, Washington, DC, pp. 1828–1833.